Ultrasonics Sonochemistry 112 (2025) 107178

Contents lists available at ScienceDirect

Ultrasonics Sonochemistry

journal homepage: www.elsevier.com/locate/ultson

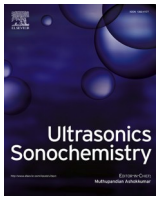

The storage quality and transcriptome analysis of fresh-cut taro by L-ascorbic acid combined with ultrasonic treatment

Lin Chen [a,1], Bingzhi Chen [a,b,1], Lulu Chu [a], Lili Chen [a], Luyu Xie [c,*], Youjin Deng [b,d,**], Yuji Jiang [a,b,***]

[a] College of Food Science, Fujian Agriculture and Forestry University, Fuzhou 350002, China
[b] Mycological Research Center, Fujian Agriculture and Forestry University, Fuzhou 350002, China
[c] Institute of Dataspace, Hefei Comprehensive National Science Center, Hefei 230000, China
[d] College of Life Science, Fujian Agriculture and Forestry University, Fuzhou 350002, China

ARTICLE INFO

Keywords:
L-ascorbic acid
Ultrasonic treatment
Fresh-cut taro
Storage quality
Transcriptome analysis

ABSTRACT

Fresh-cut taro, renowned for its high nutritional value and convenience, is prone to rapid browning post-cutting, which hinders its storage life. This study focused on the effects of L-ascorbic acid (AA) combined with ultrasound (US) treatment (AS) on the storage quality and transcriptome analysis of fresh-cut slices of Yongding June Red Taro. Compared to the control (CK) group, AS treatment effectively reduced the weight loss rate of taro slices, maintained higher hardness, delayed the increase of browning, and inhibited the accumulation of O_2^- and H_2O_2. Furthermore, the AS group showed increased glutathione levels and maintained higher activities of ascorbate peroxidase and glutathione reductase, yet decreased the contents of flavonoids and reducing sugars. Simultaneously, in the AS group, the activities of tyrosinase and lipoxygenase were lowered, thereby preserving the high sensory quality of fresh-cut taro slices. Transcriptome analysis revealed that differentially expressed genes (DEGs) between the AS and CK groups were annotated and categorized into 50 and 20 functional groups based on the Gene Ontology (GO) and Kyoto Encyclopedia of Genes and Genomes (KEGG) databases, respectively. Notably, both groups exhibited significant enrichment in processes related to photosynthesis, protein processing in the endoplasmic reticulum, and isoflavone biosynthesis. Therefore, we concluded that AS treatment could alleviate oxidative stress and maintain storage quality by regulating metabolic pathways. These findings provide insights into the physiological changes occurring in taro immediately after cutting and serve as an essential basis for developing effective storage and preservation techniques.

1. Introduction

Colocasia esculenta (L.) Schott, commonly known as taro, is a monocotyledonous perennial herb belonging to Araceae. It is widely cultivated in Chinese regions such as Yunnan, Sichuan, and Fujian [1]. As a National Geographic Indication product, June Red Taro stands out as a novel variety, bred from the white bud taro varieties nurtured by local farmers in Yongding District, Longyan City, Fujian Province, China. It is celebrated for its early maturation, superior quality, and abundant yield.

In recent years, fresh-cut fruit and vegetables have gained popularity among consumers for their natural flavors and convenience [2,3]. Fresh-cut taro, being more easily consumable, faces issues such as tissue disruption, cut surface browning, and skin irritation upon handling, which can hinder consumption, reduce nutritional value, and limit shelf life [4]. These challenges pose a significant problem for the fresh-cut taro industry and emphasize the need for effective methods to prevent browning during storage and consumption. However, few studies have explored the application of L-ascorbic acid (AA) combined with ultrasound (US) treatment (AS) for color preservation in fresh-cut taro. Current research on fresh-cut taro primarily focuses on several key areas: the evaluation of storage techniques [5]; the investigation of

* Corresponding author.
** Corresponding author at: Mycological Research Center, Fujian Agriculture and Forestry University, Fuzhou 350002, China.
*** Corresponding authors at: College of Food Science, Fujian Agriculture and Forestry University, Fuzhou 350002, China.
E-mail addresses: x86@u.nus.edu (L. Xie), dengyoujin1980@163.com (Y. Deng), jyj1209@163.com (Y. Jiang).
[1] These authors contributed equally to this paper.

https://doi.org/10.1016/j.ultsonch.2024.107178
Received 10 September 2024; Received in revised form 30 October 2024; Accepted 25 November 2024
Available online 27 November 2024

browning characteristics [6,7]; the impact of cutting on the physiological and biochemical qualities [8]; and the application of taro slime in preservation [9]. Notably, there is limited research into the molecular mechanisms behind browning in fresh-cut taro. Therefore, this study aimed to investigate the effects of AS treatment on the storage quality of fresh-cut taro and to elucidate the browning mechanism through transcriptomics.

Transcriptome sequencing has been extensively employed in various organisms across diverse environments [10–15]. In this study, we used June Red Taro as the material, analysed the gene expression differences between the treatment and the control (CK) group by transcriptomics, and combined with bioinformatics to reveal the browning mechanism of fresh-cut taro. Our findings offer valuable insights into the mechanisms underlying the quality changes in fresh-cut taro during storage, thereby facilitating the development of effective preservation techniques.

2. Materials and methods

2.1. Experimental materials

June Red Taro specimens were sourced from the Agricultural Technology Station, Yongding District, Longyan City, Fujian Province, China. On the specific day of collection, specimens of uniform size, intact appearance, and free from damage (mechanical and insect) were carefully selected for storage. They were packed and promptly delivered to the Mycological Research Center of Fujian Agriculture and Forestry University.

2.2. Sample treatment

For AS treatment, the taros were peeled, washed, and cut into 3–5 mm thick slices. The slices were then soaked in a 2 % mass fraction AA solution for 15 min. After natural drying, they were vacuum-packed at −60 kPa, with three slices per vacuum bag of 15 × 20 cm, 0.19 mm thickness, and nylon texture (Cundi Flagship Store, Fujian, China). The bags were subsequently immersed in water in an SK8210LHC ultrasonic cleaner (Shanghai Kudos Ultrasonic Instrument Co. Ltd., China), treated with US at 53 kHz, 400 W, water bath (30 ℃) for 10 min. Finally, the bags were removed, the water stains on the bag surfaces were wiped off, and stored at 4 ± 0.5 ℃ for 20 d. The samples in the CK group were not soaked in AA solution and treated with US, and stored under the same conditions as the AS group. On days 0, 4, 8, 12, 16, and 20, 3 bags of samples were taken from AS group and CK group, and the relevant indexes were measured, and 3 replicates were set for each group. The remanent samples were frozen in liquid nitrogen and stored at −80 ℃ for browning-related enzyme activity analysis, RNA sequencing, and qRT-PCR verification. Among them, the samples for RNA sequencing were sent to the Metville Biotechnology Co., Ltd. (Wuhan, China) for gene expression analysis.

2.3. Determination of weight loss rate, browning degree, and hardness of fresh-cut taro

The weight loss rate was determined by reference to a previous method [16]. Weight loss rate (%) = $[(m_1\text{-}m_2)/m_1] \times 100$, where m_1 represents initial weight (g) on day 0, and m_2 is the weight (g) on day 4, 8, 12, 16, and 20.

The L* (light / dark), a* (red / green), and b* (yellow / blue) values were measured by DCI-60-C automatic colometry (Beijing Chenteck Instrument Technology Co., Ltd. China) every 4 days during storage at 4 ℃ [17] and then the BD value was determined using the method of Badin et al. according to Eq. (1) [18]. The BD value reflects the the surface color (Browning degree) of the fresh-cut taro.

$$BD = 100(X - 0.31)/0.172 \quad (1)$$

Where X=(a*+1.75L*)/(5.645L*+a*-3.012b*).

The hardness was determined using a TA.XT Plus C physical property tester (Stable Micro Systems Company, UK) and P5 cylindrical probe in TPA mode [19]. And the test mode was TPA, the rate was 2 mm/s before, during and after the test, the depth was 5 mm, the unit was N, the hardness I was taken as the index, and the results obtained were taken as the average value.

2.4. Determination of the activities of browning-related enzymes in fresh-cut taro

The activities of tyrosinase (TYR), ascorbate peroxidase (APX), glutathione reductase (GR), and lipoxygenase (LOX), as well as the contents of glutathione (GSH), superoxide anions (O_2^-), hydrogen peroxide (H_2O_2), flavonoids, and reducing sugars were determined following the instructions provided by the corresponding kits (Beijing Solarbio Science & Technology Co. Ltd., Beijing, China).

For TYR and GR determination, 0.1 g of frozen taro tissue was homogenized in an ice bath with 1 mL of extraction solution from the assay kits and centrifuged at 10,000 g at 4 ℃ for 10 min. Then, the supernatant was processed by adding assay kit reagents. Finally, the TYR and GR activities were measured in absorbance of 505 nm and 340 nm, respectively, expressed as U. One TYR activity unit (U) was defined as a change of 0.01 in absorbance value at 505 nm per minute per g of tissue in the reaction system. One GR activity unit (U) was defined as catalyzing 1 μmol of NADPH oxidation per minute per gram of sample at 37 °C, pH 8.0.

For APX and LOX determination, 0.1 g of frozen taro tissue was homogenized in ice bath with 1 mL of extraction solution from the assay kits and centrifuged at 13,000 g at 4 ℃ for 20 min. Then, the supernatant was processed by adding assay kit reagents. Finally, the APX and LOX activities were measured in absorbance of 290 nm and 234 nm, respectively, expressed as U. One APX activity unit (U) was defined as 1 μmol of AsA oxidized per minute per g of tissue. One LOX activity unit (U) was defined as a change of 0.001 of catalytic absorbance per minute per gram of sample at 25°C in a 1 mL system.

For H_2O_2 determination, 0.1 g of frozen taro tissue was homogenized in ice bath with 1 mL of reagent one from the assay kit and centrifuged at 8000 g at 4 ℃ for 10 min. Then, the supernatant was processed by adding assay kit reagents. Finally, the H_2O_2 content was measured in absorbance of 415 nm, expressed as mmol kg^{-1}.

For O_2^- determination, 0.1 g of frozen taro tissue was homogenized with 1 mL of extraction solution from the assay kit and centrifuged at 12,000 g at 4 ℃ for 20 min. Then, the supernatant was processed by adding assay kit reagents. Finally, the O_2^- content was measured in absorbance of 530 nm, expressed as mmol kg^{-1}.

For GSH determination, 0.1 g of frozen taro tissue was homogenized in ice bath with 1 mL of reagent one from the assay kit and centrifuged at 12,000 g at 4 ℃ for 10 min. Then, the supernatant was processed by adding assay kit reagents. Finally, the GSH content was measured in absorbance of 412 nm, expressed as mg kg^{-1}.

For flavonoid determination, 0.1 g of frozen taro tissue was extracted with 1 mL of extraction solution from the assay kit for 30 min at ultrasonic power of 300 W and temperature of 60°C, followed by centrifugation at 12,000 g at 25 °C for 10 min. Then, the supernatant was processed by adding assay kit reagents. Finally, the flavonoid content was measured in absorbance of 470 nm, expressed as g kg^{-1}.

For reducing sugar determination, 0.1 g of frozen taro tissue was homogenized in ice bath with 1 mL of reagent one from the assay kit, followed by incubation in a water bath at 80 °C for 40 min. After that, it was removed and mixed by turning up and down 8–10 times, then centrifuged at 8000 g at 25 °C for 10 min. Subsequently, the supernatant was processed by adding assay kit reagents. Finally, the reducing sugar content was measured in absorbance of 540 nm, expressed as mg kg^{-1}.

2.5. RNA extraction, library construction, and data quality control

Total RNA was extracted by employing the E.Z.N.A. Plant RNA kit (Omega Bio-Tek, GA, USA) according to the instructions. The RNA purity was confirmed using a NanoPhotometer by estimating the $OD_{260/280}$ and $OD_{260/230}$ ratios. The RNA concentration and integrity were determined utilizing a Qubit2.0 fluorometer and an Agilent 2100 bioanalyzer, respectively.

After RNA detection, Wuhan Metville Biotechnology Co., Ltd. constructed the transcriptome library and conducted rigorous quality inspections. Upon meeting our specific standards, qRT-PCR was used to precisely and effectively measure the library concentration, thus ensuring high quality.

The raw data was meticulously filtered using fastp, primarily to eliminate the adapter-containing reads. Paired-end reads were discarded if the "N" content or the number of low-quality bases ($Q \leq 20$) exceeded 10 % and 50 % of the total base count, respectively. All subsequent analyses were conducted solely on the clean reads, ensuring data accuracy and reliability.

2.6. Differentially expressed genes (DEGs) and enrichment analysis

DEGs between the two groups were recognized using DESeq2 and corrected for P-values by applying the Benjamini & Hochberg method. The genes with $[\log_2(\text{fold change})] \geq 1$ and $P < 0.05$ were identified as the significant DEGs. Further, enrichment analysis of the DEGs was performed based on the hypergeometric test. For the Kyoto Encyclopedia of Genes and Genomes (KEGG) pathway, the hypergeometric distribution test was conducted in terms of the pathways. For Gene Ontology (GO), enrichment analysis was performed based on the GO terms.

2.7. qRT-PCR analysis

Primers specific for five target genes were designed using the Primer Premier 5.0 software, and the *Nascent Polypeptide-Associated Complex Subunit* (*NPC-B*) was the internal reference gene (Table 1). cDNA was synthesized using the TransScript® Uni All-in-One First-Strand cDNA Synthesis SuperMix for qPCR (One-Step gDNA Removal) kit (Transgen Biotech Co., Beijing, China), with 1000 ng of the total RNA as the template. For qRT-PCR, a real-time fluorescence quantitative kit was employed; the 20 μL reaction mixture contained 2 μL of template RNA, 0.4 μL of forward and reverse primers, 10 μL of 2 × PerfectStart® Green qPCR SuperMix, and nuclease-free water. The thermal cycling program comprised an initial denaturation step at 94 °C for 30 s, followed by 40 cycles of denaturation at 94 °C for 5 s, and annealing at 60 °C for 30 s; triplicates per sample.

2.8. Statistical analysis of the data

The experimental data were analyzed and processed by employing the GraphPad Prism software. The significance level was 0.05, and three parallels were set in each group. The results were expressed as the mean ± standard deviation.

Table 1
Sequences of the gene-specific primers used for real-time quantitative PCR.

Gene name	Forward primer (5′→3′)	Reverse primer (5′→3′)
NPC-B	ATGGGTTGTTAGCGGCTCT	ATCTGCTCCGCCAACTTCT
EVM0019478	GTCTTCGACCCTTTCTCTCT	ACCTTCACCTCTTCCTTGT
EVM0027930	GACTCCTACGCCTTCGT	AAGTACTGCCCTCCTTGT
EVM0027993	CGAGGTCAAGATCGCATAAC	GGAGAGAACGCACAAGAAA
EVM0023132	ATGTCGATCGTCCCTAGTT	ACCTTAACCTCCTCCTTCTT
novel.3152	GGAGAGAACGCACAAGAAA	CGAGGTCAAGATCGCATAAC

3. Results

3.1. AS treatment actively impacts the sensory quality and browning degree of fresh-cut taro

During storage, fresh-cut taro in the CK group gradually browned and dehydrated. However, there was no significant change in the AS group throughout the storage period (Fig. 1). After 8 d, the CK group displayed conspicuous browning, unlike the AS group. After 20 d, the CK group exhibited wrinkled and cracked features in addition to browning. In contrast, the AS group only exhibited minor browning at the edges, without any visible signs of surface wrinkling or cracking.

The browning degree exhibited a consistent enhancement as the storage duration was prolonged (Fig. 2A). However, compared to the CK group, the browning degree in the AS group was markedly lower ($P < 0.01$). On day 20, the browning degree in the AS group was 11.5, representing a 47 % reduction compared to that of the CK group of 21.6, indicating a remarkable difference ($P < 0.01$).

3.2. AS treatment proactively impacts the weight loss rate and hardness of fresh-cut taro

A significant factor contributing to the elevated respiratory and transpiration rates in fresh-cut taro is the mechanical damage incurred during the slicing process. Consequently, the weight loss rate gradually increases during storage (Fig. 2B). Notably, after 16 d, the weight loss rate of AS-treated taro was significantly lesser compared to the CK group ($P < 0.05$).

Hardness, a crucial indicator that directly reflects the quality of fruit and vegetables, significantly impacts consumer acceptance [20]. During storage, the hardness of fresh-cut taro in the various groups declined, but more rapidly in the CK than in the treatment groups (Fig. 2C). Notably, the hardness in the AS group was evidently higher than the CK group on days 4 and 12 ($P < 0.05$) and after 16 d ($P < 0.01$). On day 20, the hardness value of the CK group was 15.5, whereas it was 17.5 in the AS group. These results clearly demonstrate that AS treatment effectively delayed the reduction in hardness and extended the shelf life of fresh-cut taro.

3.3. AS treatment evidently impacts the active oxygen metabolism of fresh-cut taro

O_2^- and H_2O_2 are two highly destructive reactive oxygen species (ROS), the excessive accumulation of which triggers the peroxidation of membrane lipids. The O_2^- content of fresh-cut taro in the CK group peaked at 0.09 mmol g^{-1} on day 12 and differed remarkably ($P < 0.01$) from the AS group at 12 d (Fig. 2D). Similarly, the H_2O_2 levels in the CK group remained consistently higher than that in the AS group throughout the storage period (Fig. 2E), with a marked increase ($P < 0.01$) after 12 d. In summary, compared to the CK group, AS treatment effectively mitigates the accumulation of O_2^- and H_2O_2 during storage, maintains the ROS metabolism balance.

3.4. AS treatment proactively impacts the GSH, flavonoid, and reducing sugar contents in fresh-cut taro

GSH serves as a crucial non-enzymatic antioxidant of the ascorbic acid-glutathione (AsA-GSH) cycle, playing a pivotal role in safeguarding fruit and vegetable tissues from oxidative stress-induced damage [21]. Compared to the CK group (Fig. 2F), AS treatment resulted in elevated levels of GSH in fresh-cut taro throughout storage, especially after 12 d, which varied significantly ($P < 0.01$) from the CK group.

In fresh-cut fruit and vegetables, flavonoid content rises over time with color intensity [22]. During storage, flavonoid levels initially increase but later decline (Fig. 2G) due to preliminary stress from cutting. On days 12 and 16, the flavonoid content of the CK group was

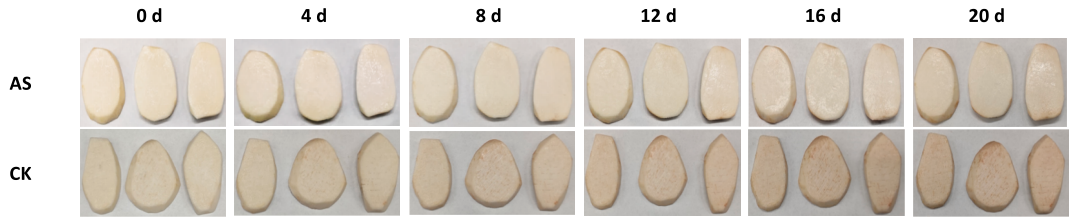

Fig. 1. AS treatment proactively impacts the appearance of fresh-cut taro. AS: combined L-ascorbic acid and ultrasonic treatment; CK: control.

remarkably more than the AS group ($P < 0.01$).

Delaying the accumulation of reducing sugars is crucial for extending the shelf-life of fresh-cut taro [23]. The reducing sugar content in fresh-cut taro enhanced with storage (Fig. 2H) more considerably in the CK compared to the AS group ($P < 0.01$).

3.5. AS treatment markedly impacts the activities of antioxidant enzymes and lipoxygenase in fresh-cut taro

TYR, a crucial rate-limiting enzyme in melanin biosynthesis [24], is a focus for research on regulating melanin production and accumulation via its inhibition [25]. On day 12, TYR activity was remarkably higher in the CK than in the AS group ($P < 0.01$) (Fig. 2I). APX and GR, critical enzymes in the AsA-GSH cycle, stabilize the GSH content [26]. In the AS group, APX and GR activities were consistently elevated than those in the CK group throughout storage (Fig. 2J-K). Compared to the CK group, the APX activity in the AS group was significantly enhanced on 8, 12, and 20 d ($P < 0.01$). There was a highly conspicuous variation between the GR activities of the AS and CK groups during the period of 4–12 d ($P < 0.01$) and on day 20 ($P < 0.05$). These results suggest that AS treatment effectively enhances APX and GR activities. The activity of LOX, a key enzyme affecting cell membrane degradation, was remarkably lesser in the AS compared to the CK group throughout storage ($P < 0.01$) (Fig. 2L).

In summary, AS treatment of fresh-cut taro effectively inhibits TYR and LOX activities, enhances APX and GR activities, and delays cell membrane degradation and aging.

3.6. RNA-seq data quality analysis and comparison with reference genomes

Based on the preliminary test results, the quality degradation of fresh-cut taro began after 12 d, marking a critical time point in determining preservation effectiveness. Consequently, in this experiment, samples were collected on days 0, 12, and 20 and labeled accordingly, and three biological replicates were set up.

The RNA isolated from the Taro samples was sequenced on Illumina, and fastp [27] was utilized for data quality control to ensure the integrity of library construction and sequencing [28]. Transcriptome sequencing of 15 samples across different storage durations yielded 729.91 million raw reads, filtered to obtain 709.49 million reads. GC content ranged from 50.12 % to 52.39 %, with Q20 base ratios > 96 % and Q30 base ratios > 91 %, indicating high-quality sequencing data suitable for further analysis (Table 2).

Using HISAT2 [29], clean reads were aligned to the reference genome to obtain genome location information and sequence-specific features of the sequenced samples. The clean reads across groups were aligned (Supplementary Table S1). All samples exhibited alignment rates > 85 % reads mapped [30] and 77 % unique mapped, demonstrating comprehensive transcriptome annotation and reliable RNA-seq data.

3.7. Gene expression analysis

FPKM (Fragments Per Kilobase of transcript per Million fragments mapped), which quantifies the transcripts or gene expression levels, effectively reflecting the variation in them among treatment groups [31]. The gene expression of fresh-cut taro on days 12 and 20 was significantly lower than that on day 0, indicating that the expression of some genes changed with the extension of storage duration (Fig. 3). This decrease may be attributed to the downregulation of genes involved in specific functional pathways or biological processes, or the regulatory role of specific transcription factors [32].

3.8. Principal component analysis (PCA) and correlation analysis among the samples

The correlation coefficient (R^2) of gene expression levels across three biological replicates in both the CK and AS groups was > 0.87 (Fig. 4A), demonstrating high reproducibility under identical conditions [33] and ensuring reliable subsequent differential gene analysis. PCA revealed good repeatability among samples and remarkable variations in sequencing outcomes among the treatments and storage durations, fulfilling analytical requirements (Fig. 4B).

3.9. Analysis of differential gene expression among samples

Using DESeq2 [34,35], variable gene expression was analyzed, and genes with $|\log2\text{Fold Change}| \geq 1$ and FDR < 0.05 were identified as differentially expressed (DEGs) (Supplementary Fig. S1). Among the 15 samples, 45,935 DEGs were identified, including 27,132 up- and 18,803 down-regulated genes.

A comparative volcano map of the differential gene expression levels between the treatment and CK groups on days 0, 12, and 20 was plotted (Fig. 5). Compared with day 0, the expression levels of 7,437 and 7,051 genes altered significantly in the CK and treatment groups on day 12 of storage, respectively. Of these, 5,086 and 4,715 genes were up-regulated, and 2,351 and 2,336 genes were down-regulated in the CK and treatment groups, respectively. On day 20, the expression of 9,879 and 9,087 genes changed markedly. Of these, 6,416 and 5,765 genes were up-regulated, and 3,463 and 3,322 genes were down-regulated in the CK and treatment groups, respectively. In summary, the up-regulated genes were greater in number than the down-regulated ones in the CK and treatment groups. In the treatment vs. CK group, on day 12, the expression of 1,795 genes changed conspicuously; 572 were up-regulated, and 1,223 were down-regulated; on day 20, a total of 2,523 DEGs were identified; 876 were up-regulated, and 1,647 were down-regulated. Thus, the down-regulated genes were greater in number than the up-regulated ones, and the number of DEGs was enhanced on day 20 compared with that on day 12.

A Venn diagram effectively illustrating the DEGs overlapping among treatment groups was plotted, allowing the identification of common or unique DEGs across different treatments (Fig. 6). On day 12, a total of 5,179 DEGs were shared between the CK-12_vs_CK-0 and T-12_vs_CK-0 comparisons, of which 539 were identical to the DEGs obtained from the T-12_vs_CK-12 comparison. On day 20, among the DEGs obtained from the CK-20_vs_CK-0 and T-20_vs_CK-0 comparisons, 6,826 were shared, of which 876 were identical to those derived from the T-20_vs_CK-20 comparison. Overall, as storage time prolonged, the number of DEGs common to the treatment and CK groups increased

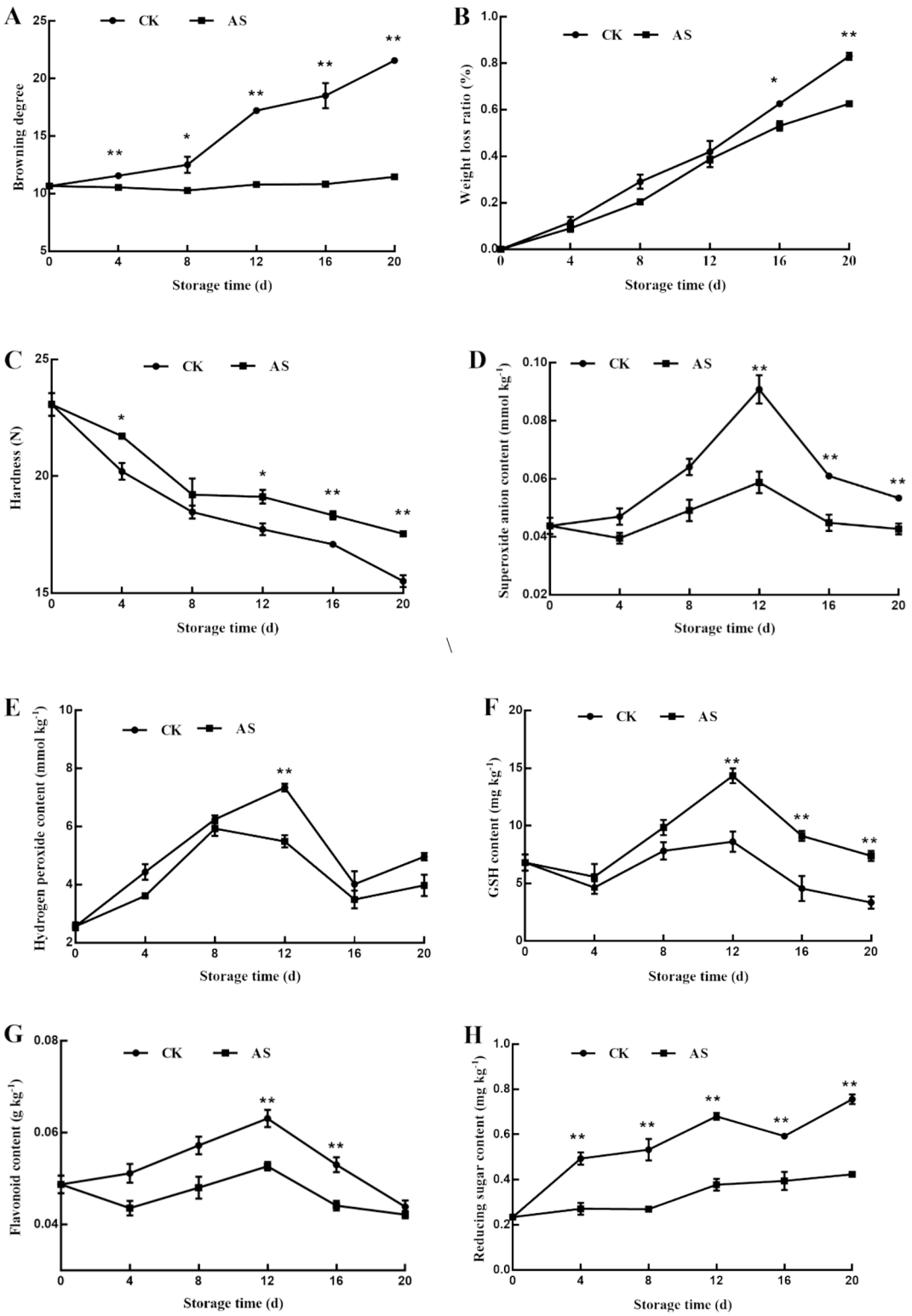

Fig. 2. The physiological indices of fresh-cut and AS-treated taro during storage. (A) Browning degree. (B) Weight loss rate. (C) Hardness. (D) Superoxide anion levels. (E) Hydrogen peroxide levels. (F) GSH content. (G) Flavonoid content. (H) Reducing sugar content. (I) TYR enzyme activity. (J) APX enzyme activity. (K) GR content. (L) LOX enzyme activity. *difference was significant ($P < 0.05$); **difference was extremely significant ($P < 0.01$) at the same storage time.

compared to those on day 0.

Clustering heat maps constructed for the DEGs of all the individual and comparative groups revealed high similarity in the gene expression patterns within the same treatment group (Fig. 7). Additionally, the three biological replicates clustered within the same category, indicating data consistency and reliability. The gene expression in the samples showed large variations with different storage periods, in particular, on day 0 compared to days 12 and 20. This trend indicated that the decline in the quality of fresh-cut taro was accompanied by differential gene expression and that these DEGs may be related to AS

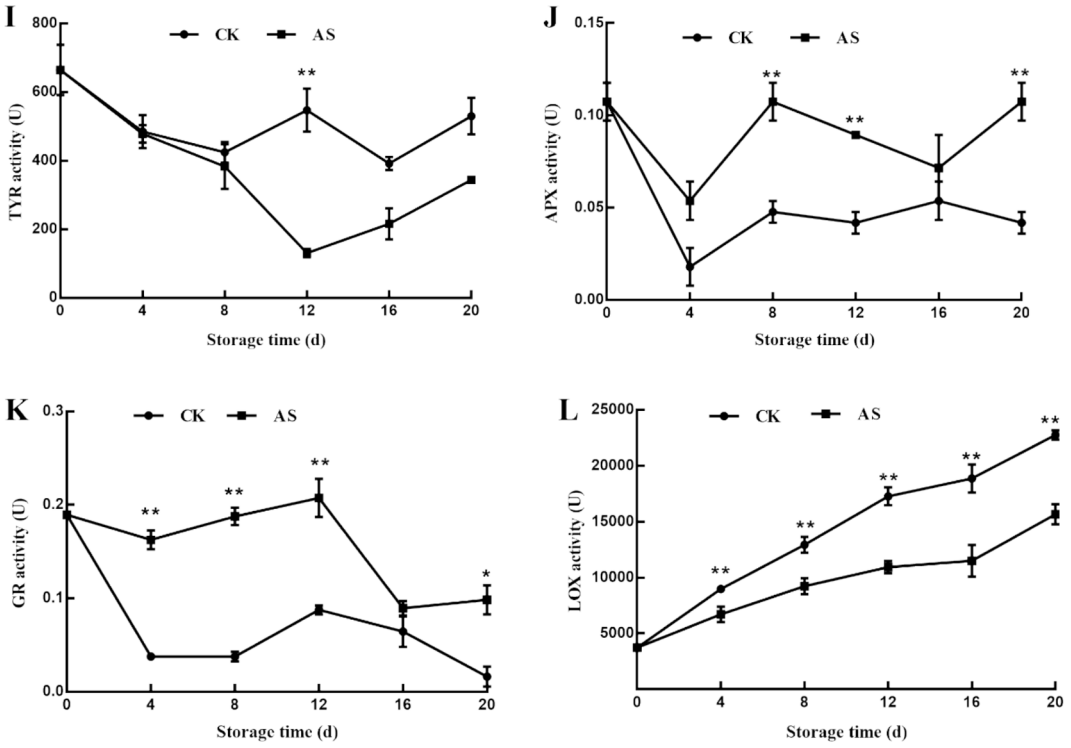

Fig. 2. (*continued*).

Table 2
RNA-Seq data of fresh-cut taro under different treatments.

Sample	Raw Reads	Clean Reads	Clean Base (G)	Error Rate (%)	Q20 (%)	Q30 (%)	GC Content (%)
CK-0–1	41,970,588	40,898,912	6.13	0.03	96.97	91.73	52.39
CK-0–2	45,800,580	44,521,808	6.68	0.03	96.99	91.78	52.19
CK-0–3	45,935,262	44,873,472	6.73	0.03	96.90	91.59	52.22
CK-12–1	49,416,858	48,066,910	7.21	0.03	96.79	91.34	50.92
CK-12–2	54,505,434	52,836,402	7.93	0.03	96.83	91.43	51.29
CK-12–3	47,221,170	45,792,090	6.87	0.03	97.16	92.16	51.39
CK-20–1	45,304,270	43,962,468	6.59	0.03	96.78	91.31	50.56
CK-20–2	49,449,446	47,822,042	7.17	0.03	96.80	91.38	50.40
CK-20–3	47,565,688	46,139,104	6.92	0.03	96.85	91.43	51.45
T-12–1	49,672,344	48,319,582	7.25	0.03	97.01	91.76	51.26
T-12–2	51,949,012	50,523,764	7.58	0.03	96.95	91.65	50.64
T-12–3	47,941,354	46,813,158	7.02	0.03	96.99	91.76	51.30
T-20–1	50,489,868	48,831,272	7.32	0.03	97.06	91.92	51.38
T-20–2	51,443,880	50,108,290	7.52	0.03	96.93	91.65	50.77
T-20–3	51,253,090	49,987,966	7.50	0.03	96.93	91.63	50.12

CK: control group; AS: treatment group. The first number indicates the storage duration. The second number represents each treatment replicate, with triplicates per group. The same applies to the following.

treatment.

These results indicated the differential expression of numerous genes in fresh-cut taro with the extension of storage duration, and the DEGs involved in the quality changes of fresh-cut taro varied with storage periods. Therefore, AS treatment affected the gene expression in fresh-cut taro to a certain extent.

3.10. GO enrichment analysis of the DEGs

GO comprises three categories: molecular function (MF), biological process (BP), and cellular component (CC). This study further categorized and enriched the DEGs between the treatment and CK groups on days 12 and 20 into these three functional classes. On day 12, the AS and CK groups shared 35, 4, and 11 common BP, CC, and MF items, respectively. The corresponding DEGs totaled 8,031; 915; and 2,773. Of these, 2,136; 246; and 752 were up-regulated, while 5,895; 669; and 2,021 were down-regulated, respectively (Supplementary Fig. S2). Notably, BP-related DEGs were primarily enriched in responses to acidic chemicals, protein folding, and photosynthesis. CC-related DEGs were mainly associated with photosynthetic, thylakoid, plastid thylakoid, and chloroplast thylakoid membranes. MF-related DEGs were primarily enriched in heme binding, unfolded protein binding, electron transfer activity, ATP-dependent protein folding chaperones, and MAP kinase kinase activity.

On day 12, DEGs were significantly enriched ($P < 0.05$) in the AS and CK groups (Fig. 8A). They were primarily associated with sulfate transport, MAP kinase activity, phosphate ion transport, jasmonate-mediated signaling, H_2O_2 response, unfolded protein binding, photosynthetic, thylakoid, plastid thylakoid, and chloroplast thylakoid membranes, as well as thermal and injury responses, and protein folding.

On day 20, DEGs were enriched in 28 BP categories (Supplementary

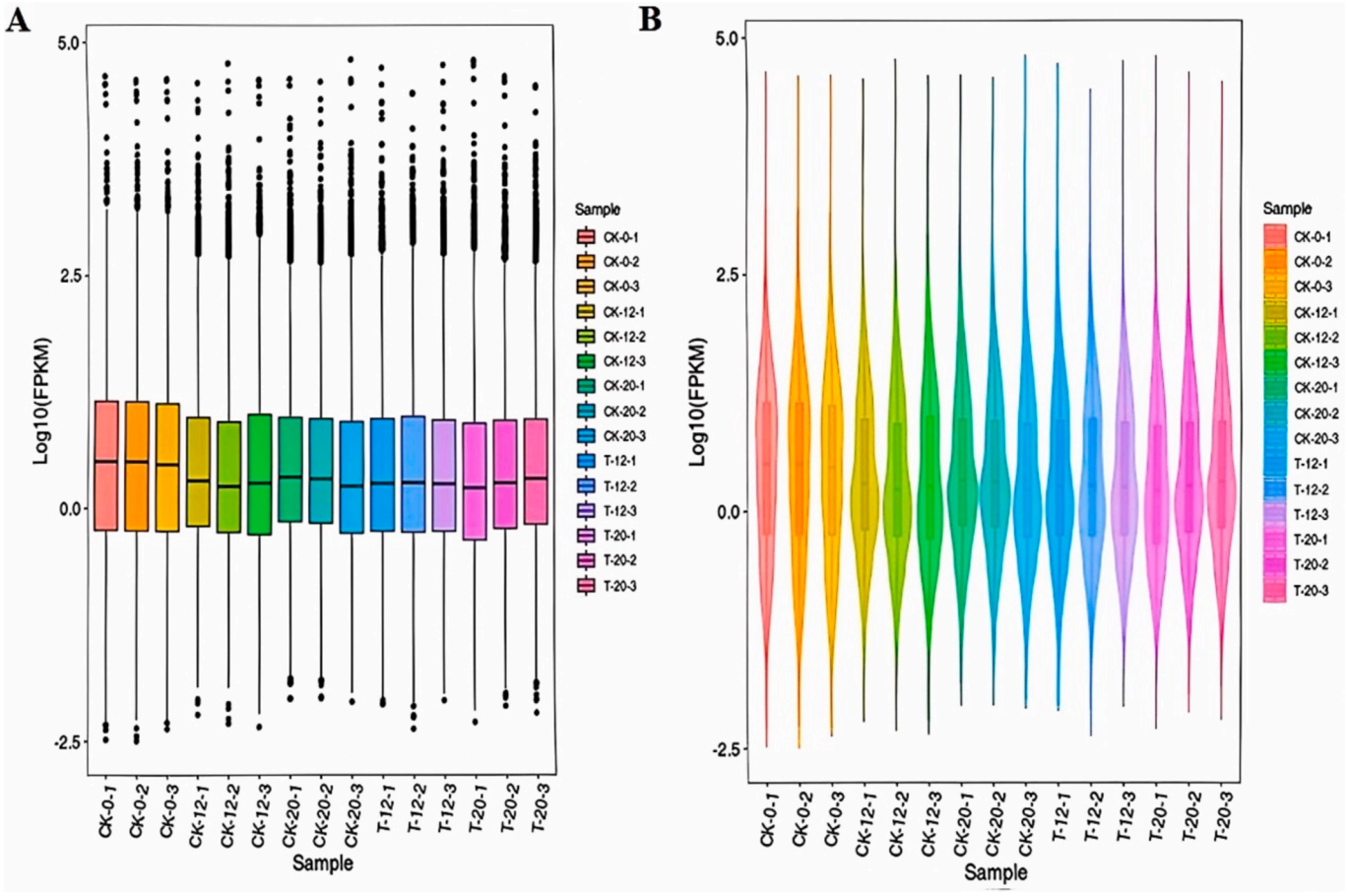

Fig. 3. Comparison of gene expression levels in the different treatment samples. A: FPKM box line diagram; B: FPKM violin diagram.

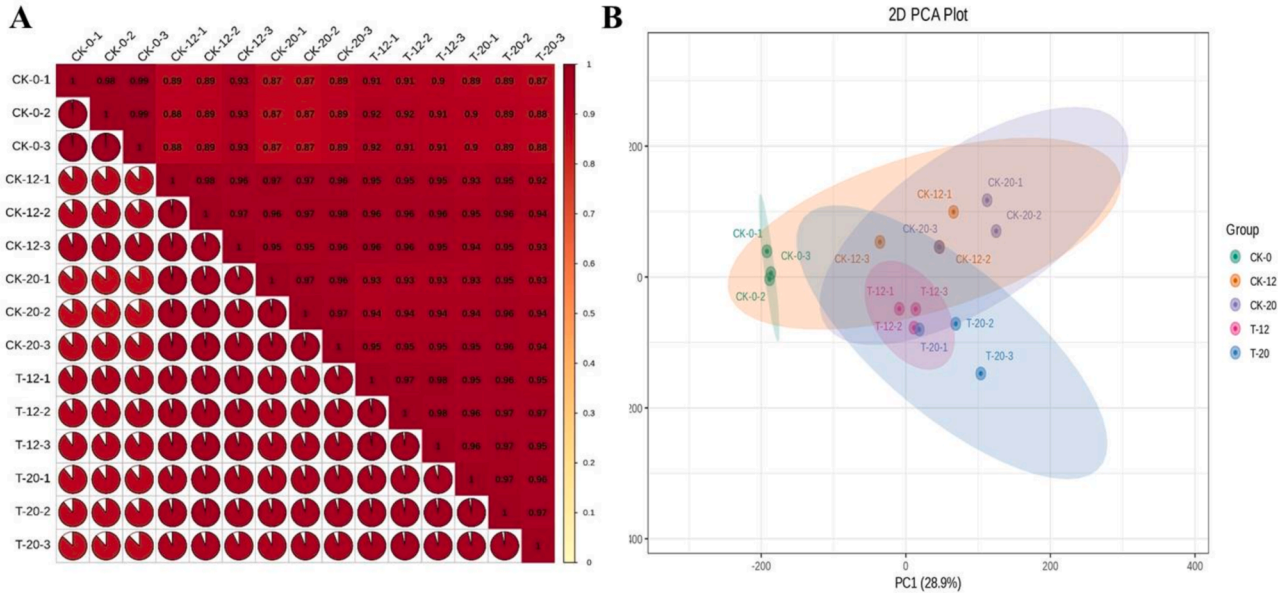

Fig. 4. Correlation (A) and principal component analyses (B) of gene expression levels among samples.

Fig. S3), representing a reduction of seven entries compared to day 12. Apart from entries consistent with those on day 12, novel enrichments included monocarboxylic acid biosynthesis, electron transport chain, and respiratory electron transport chain. Identical to those observed after 12 d, four items remained enriched in the CC category despite an increase in gene numbers and a decrease in proportion. Additionally, compared to 12 d, 18 items were enriched in the MF category, with seven novel entries encompassing primary active transmembrane transporter activity, kinase binding, isotropic transporter activity, REDOX enzyme activity acting on NAD(P)H, quinone receptor-mediated

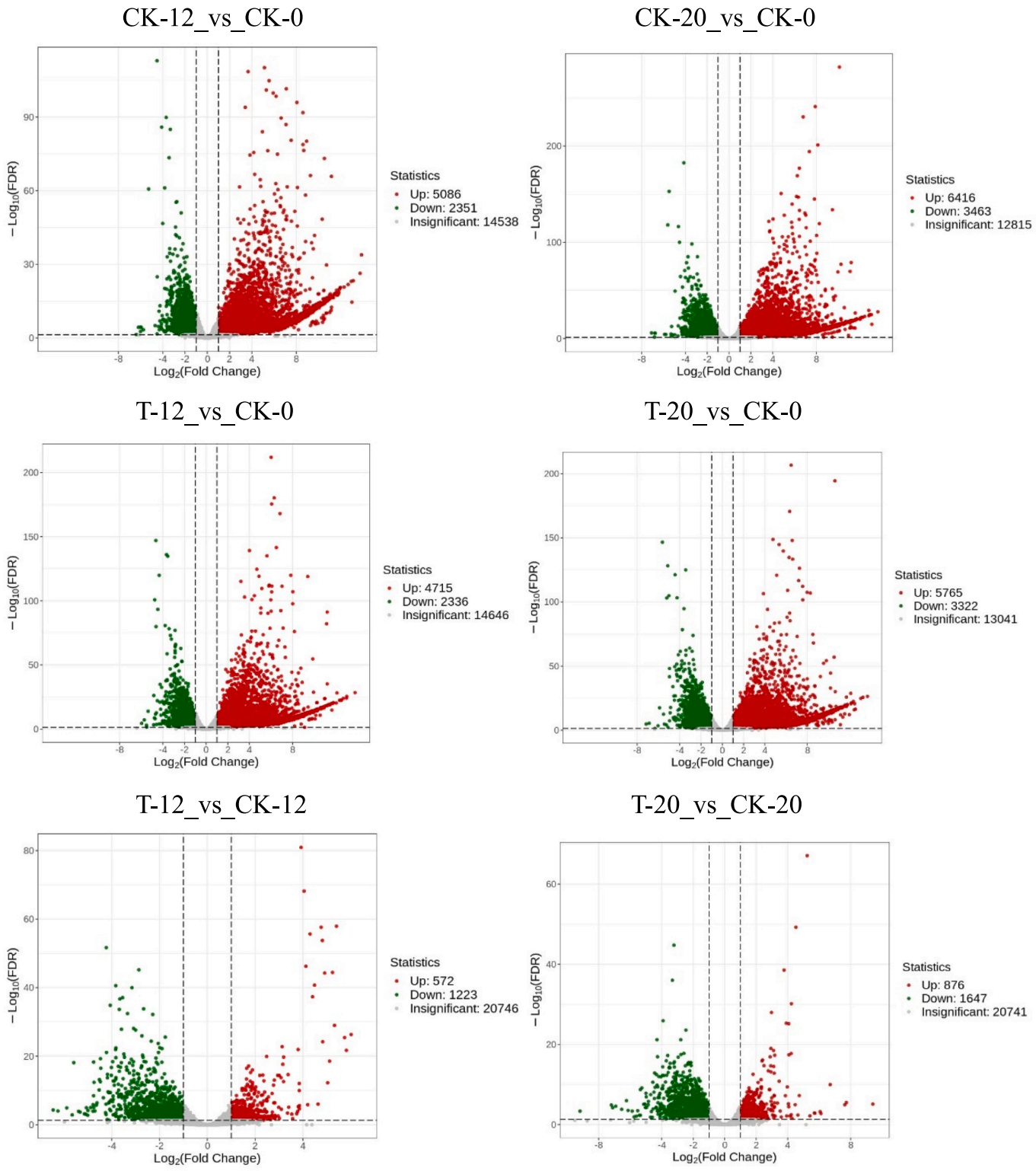

Fig. 5. A volcano map of the differentially expressed genes (DEGs). The horizontal coordinate indicates the change of gene expression multiple, and the vertical coordinate indicates the significance level of the DEGs. The red and green dots represent the up-regulated and down-regulated DEGs, respectively. The gray dots indicate the non-DEGs. (For interpretation of the references to color in this figure legend, the reader is referred to the web version of this article.)

REDOX activity, transmembrane transporter activity driven by REDOX reactions, NADH dehydrogenase activity, NAD(P)H dehydrogenase (quinone) activity, NADH dehydrogenase (quinone) activity, protein kinase binding, and NADH dehydrogenase (ubiquinone) activity.

Marked enrichment ($P < 0.05$) of DEGs was observed in the AS and CK groups after 20 d (Fig. 8B). They included phosphate ion transport, jasmonin regulation and signaling, redox-driven active transmembrane transporter activity, action on NAD(P)H, quinone or similar compounds as receptors, NADH dehydrogenase (quinone) activity, electron transfer, and components of photosynthetic membranes, including thylakoid and plastid thylakoid membranes, particularly in chloroplasts.

Upon integration of the preceding results, it was evident that the

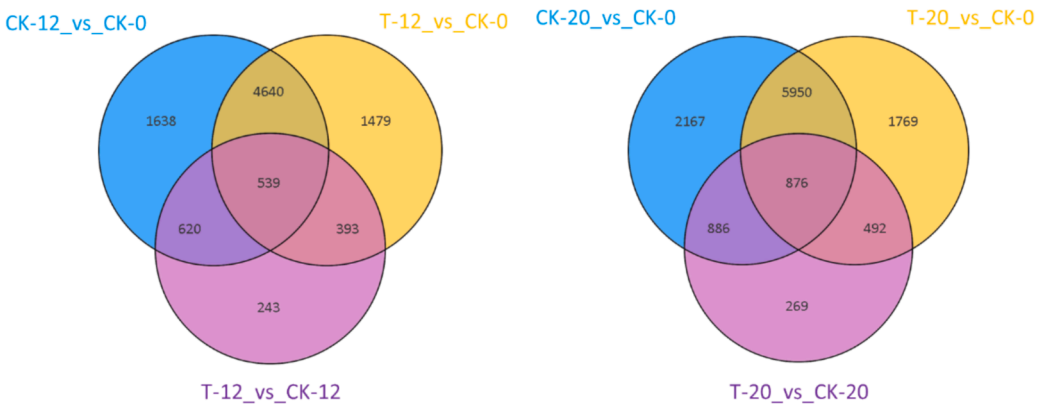

Fig. 6. Venn diagram of the differentially expressed genes (DEGs) in fresh-cut taro treated with AS and stored for varying periods. The two graphs represent the similarities and differences among the DEGs between the treatment and CK groups at 12 and 20 d, respectively, i.e., the number of co-expressed and independently expressed genes.

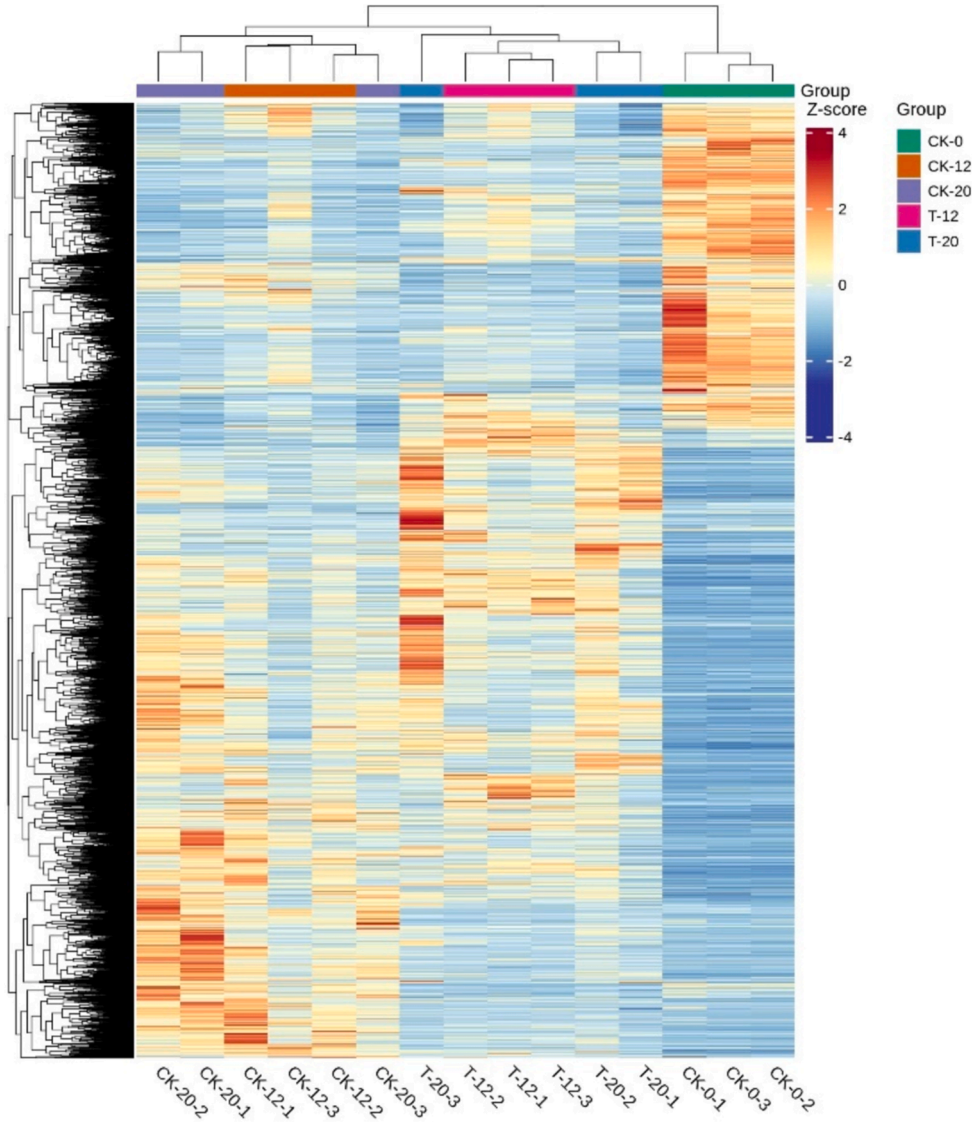

Fig. 7. A heatmap indicating the clustering of the differentially expressed genes.

DEGs in AS and CK groups were profoundly enriched in photosynthetic membranes, thylakoid membranes, plastid thylakoid membranes, and chloroplast thylakoid membranes during the storage of fresh-cut taro. Notably, protein folding-related genes were significantly enriched on 12 d, while transporter activity-related genes were enriched on 20 d. These findings suggest that the cell composition and metabolic pathways

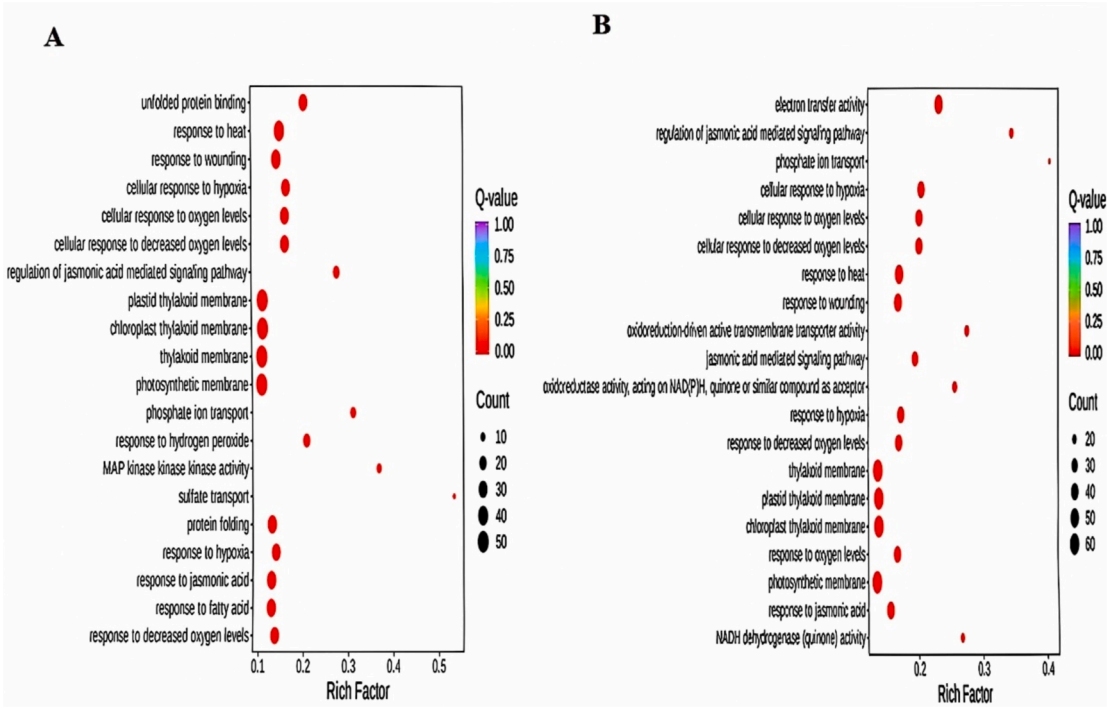

Fig. 8. Gene ontology (GO)-based functional enrichment and analysis of significant differentially expressed genes (DEGs) in the AS and CK groups on 12 (A) and 20 d (B). The 50 GO terms with the smallest q-value during the enrichment analysis were selected. If the enriched pathway entries were < 50, all were displayed. The abscissa denotes the Rich Factor; the greater the Rich Factor, the higher the degree of enrichment. The ordinate represents the GO entry; the larger the point, the more GO entries in the DEGs; the deeper the red color of the point, the more marked the enrichment. (For interpretation of the references to color in this figure legend, the reader is referred to the web version of this article.)

associated with BP were significantly altered in fresh-cut taro treated with AS.

3.11. KEGG enrichment analysis of the DEGs

The DEGs were primarily enriched in photosynthesis (Fig. 9), protein processing within the endoplasmic reticulum, isoflavone biosynthesis, metabolic pathways, flavonoid and flavonol biosynthesis, beet red

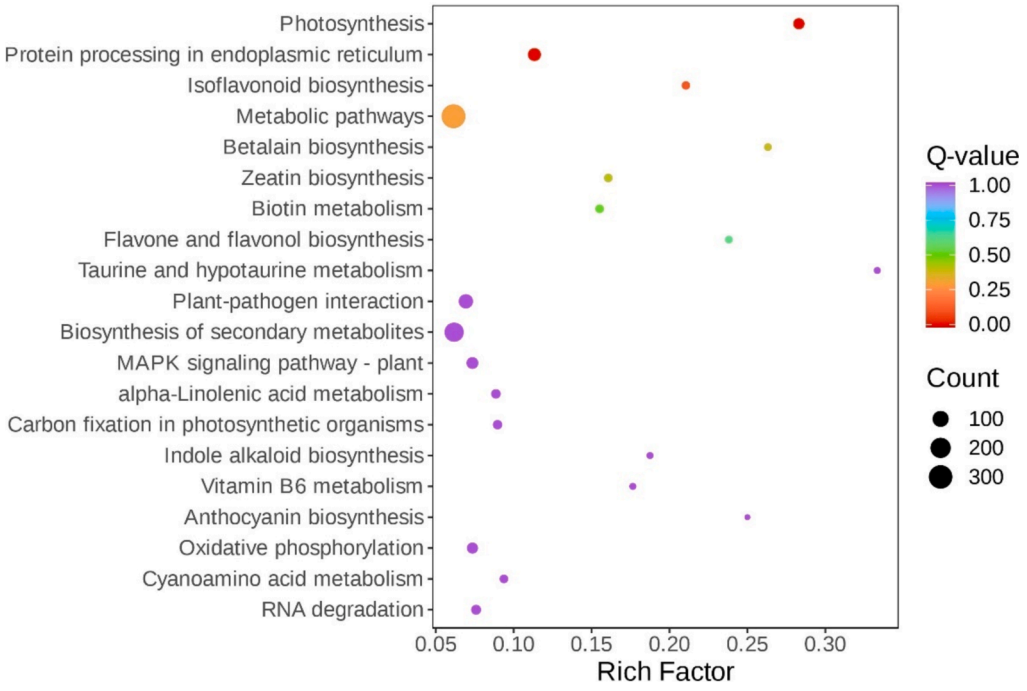

Fig. 9. Kyoto Encyclopedia of Genes and Genomes (KEGG)-based enrichment analysis of the significant differentially expressed genes between the AS treatment and control groups identified at 12 d.

pigment synthesis, zein biosynthesis, and biotin metabolic pathway.

The DEGs of the photosynthetic pathway were primarily associated with cytochrome complexes and ATP synthases (Fig. 10A). Here, four genes were up-regulated, while 26 were down-regulated, indicating photosynthesis inhibition. Chlorophyll and other photosynthetic pigments may oxidize, decompose, or transform into other compounds following fresh cutting, leading to ineffectiveness and browning. Notably, the expression of the *novel.10634* gene was the maximal (Fig. 10B), with down-regulation observed in the CK and treatment groups at 12 d. This gene encodes the photosystem II P680 reaction center D2 protein [EC: 1.10.3.9], which is crucial for light energy capture and electron transport. Its suppression indicates compromised photosynthetic efficiency, resulting in incomplete utilization of light energy. Currently, there is a paucity of reports exploring the correlation between browning and photosynthesis in fresh-cut fruit and vegetables during storage. This observation suggests that browning in fresh-cut taro during storage is specific and may result from segmentation-induced instability in photosynthesis, potentially affecting taro freshness and leading to browning.

The DEGs related to protein processing in the endoplasmic reticulum (ER) primarily centered on ribonucleic acid I, ER chaperone BiP [EC: 3.6.4.10], mannooligosaccharide α-1,2-mannosidase [EC: 3.2.1.113], ER Man9GlcNAc2 1,2-alpha-mannosidase [EC: 3.2.1.209], heat shock proteins (70 kDa 1/6/8), chaperone HtpG, DnaJ subfamily A member 1, heat shock protein 110 kDa, crystalline protein αA, Derlin-1, and E3 ubiquitin protein ligase RNF5 [EC: 2.3.2.27] (Fig. 11A). Notably, 46 genes regulating the chaperone HtpG and HSP20 family proteins were up-regulated, while five genes regulating the heat shock 70 kDa proteins, ER chaperone BiP, and Derlin-2/3 were down-regulated. This finding is consistent with previous reports on exogenous auxin up-regulating E3 ubiquitin protein ligase, which is crucial for transcriptional regulation, protein degradation, and stress responses [36]. It is speculated that the up-regulated genes enhance ER protein processing, including antioxidant defense proteins, to mitigate oxidative stress and maintain storage quality in fresh-cut taro. Additionally, 46 genes related to ER protein processing were up-regulated, while five were down-regulated (Fig. 11B). Notably, *EVM0007787S* encoding glycosyl transferase [EC: 2.4.99.18], involved in N-glycan biosynthesis and other metabolic pathways was markedly up-regulated in the CK and treatment groups at 12 d. This observation mirrors the findings on the inhibition of N-glycan synthesis in molds during *Bacillus velezensis*-based HY19 fermentation, impeding infection by the pathogen in citrus [37].

During isoflavone biosynthesis, two and six genes were up- and down-regulated, respectively (Fig. 12 A-B). They are primarily involved in the conversion of liquiritin to daidzein and the synthesis of genistein from pharmacin and naringenin. Santalane synthetase [EC: 4.2.1.139] and 2-hydroxy isoflavone dehydratase [EC: 4.2.1.105] were down-regulated (Fig. 12C). In isoflavone 7-O-glucoside-6″-O-malonyltransferase [EC: 2.3.1.115], one gene was down-regulated, while two were up-regulated. The preponderance of down-regulated genes suggests the inhibition of isoflavone biosynthesis, potentially suppressing browning in fresh-cut taro. This observation aligns with studies demonstrating melatonin's ability to suppress flavonoid synthesis gene expression, delaying browning in lotus roots [38].

In brief, KEGG functional classification and enrichment analysis revealed significant enrichment of DEGs in photosynthesis, protein processing in the ER, and isoflavone biosynthesis in both the treated and CK groups of fresh-cut taro during storage. The differential gene expression patterns had a notable influence on the storage quality of fresh-cut taro, concurring with the GO enrichment results. These pathways may represent fundamental metabolic mechanisms underlying the ability of AS treatment to preserve fresh-cut taro.

3.12. qRT-PCR verification

To further validate the transcriptome data, five up-regulated candidate genes exhibiting high expression levels and with marked differential expression were selected from the ER protein processing pathway in the AS and CK groups on 12 d for qRT-PCR (Fig. 13).

qRT-PCR demonstrated significantly higher relative expression levels of the five DEGs related to K13993 HSP20 family proteins in the AS group compared to the CK group in fresh-cut taro,which agreed with

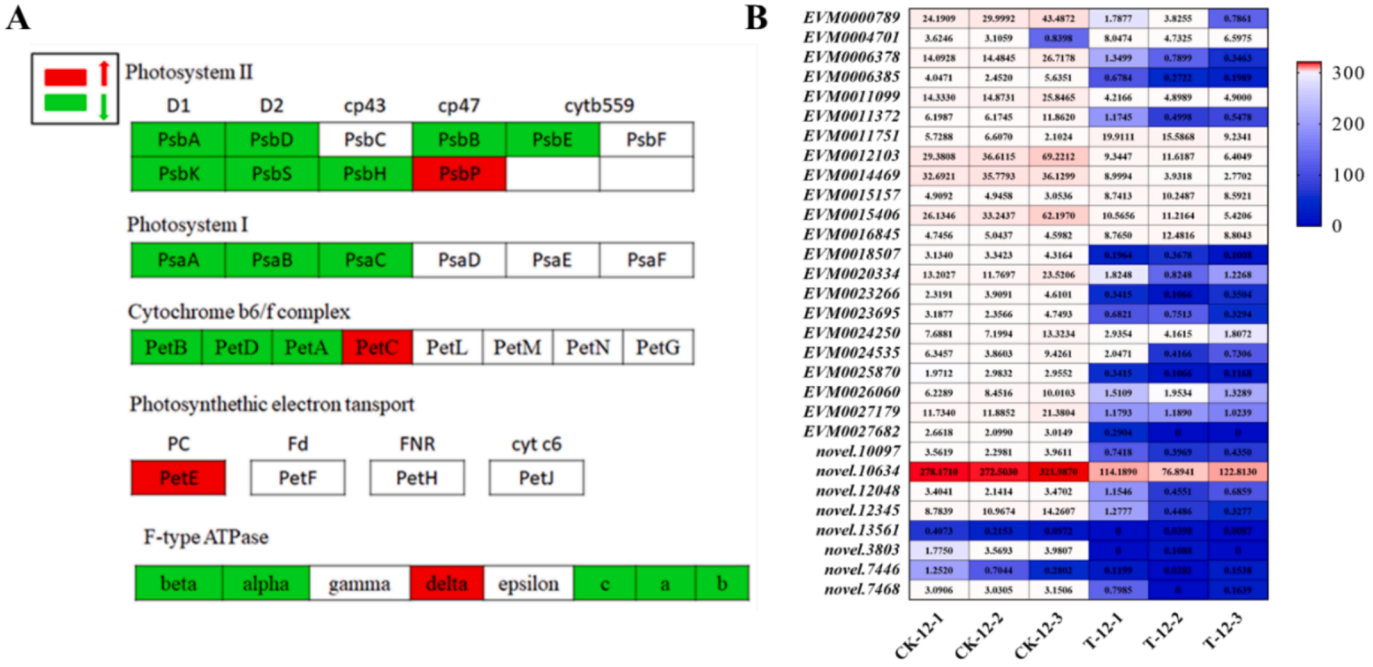

Fig. 10. The cooperative pathways and heat maps of the differentially expressed genes (DEGs) between the AS and CK groups at 12 d. A: Photosynthetic pathway, red and green boxes represent the up- and down-regulated DEGs; B: A calorimetric map of the DEGs; the more intense the red color, the higher the gene expression levels, and the more intense the blue color, the lower the gene expression levels. (For interpretation of the references to color in this figure legend, the reader is referred to the web version of this article.)

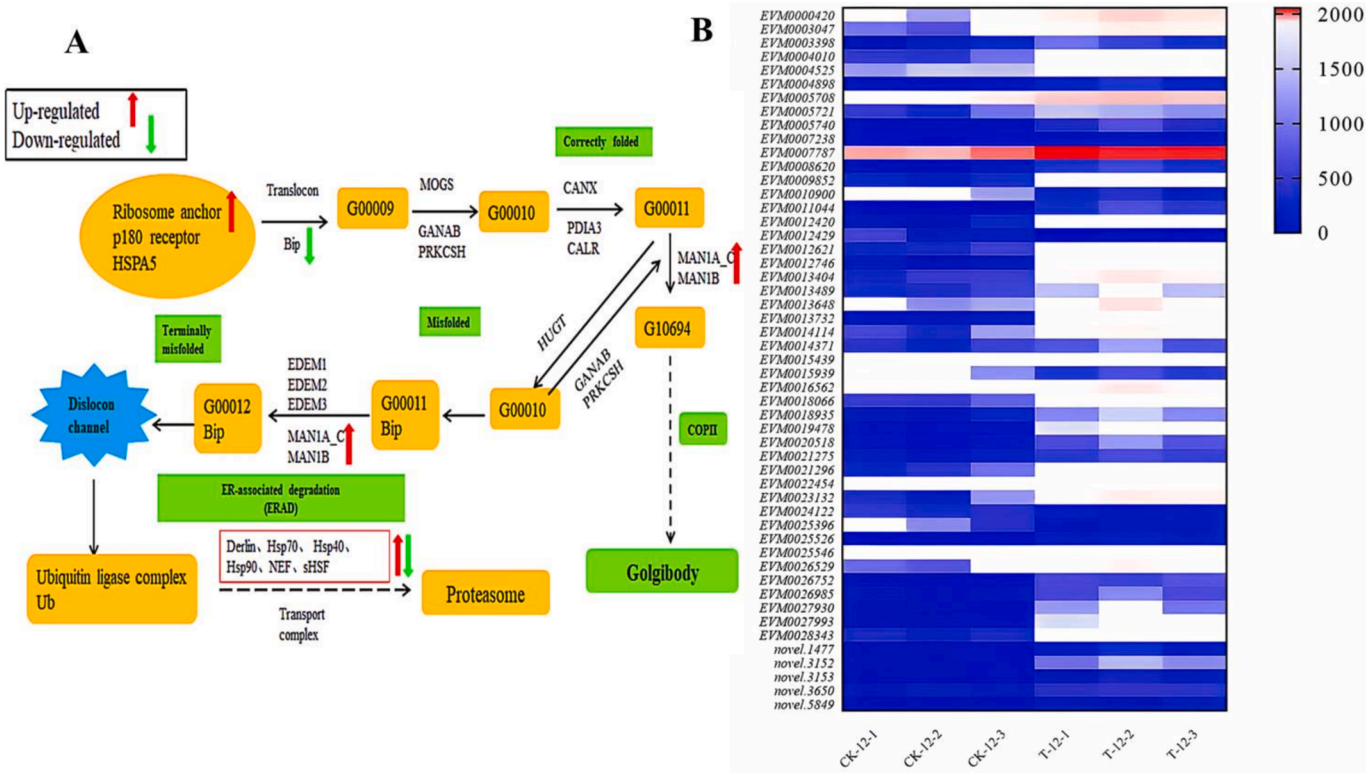

Fig. 11. Heat maps of the protein processing pathways and differentially expressed genes (DEGs) in the endoplasmic reticulum (ER) of the AS and CK groups at 12 d. A: ER protein processing pathway; red and green arrows represent the up- and down-regulated DEGs. B: A calorimetric map of the DEGs. In Figure B, the more intense the red color, the higher the gene expression level, and the more intense the blue color, the lower the gene expression level. (For interpretation of the references to color in this figure legend, the reader is referred to the web version of this article.)

the RNA-Seq data, thereby validating the reliability of the transcriptome-derived DEGs. HSP20 proteins respond to stress, and the five DEGs are also part of the ER protein processing pathway. Thus, we speculate their upregulated expression may be related to stress conditions during storage and processing, potentially contributing to protein stability and browning reduction. This result not only confirmed the reproducibility of RNA-seq result but also laid a robust foundation for further candidate gene identification and research.

3.13. Correlation analysis between the physiological characteristics of fresh-cut taro and genes of the isoflavone biosynthesis pathway after AS treatment

Correlation analysis revealed distinct patterns between the physiological traits and the isoflavone biosynthesis pathway-related DEGs (Fig. 14). Browning degree was positively correlated with *EVM0004153* ($P < 0.05$), while H_2O_2 content significantly correlated with *novel.8169* and *novel.1732* ($P < 0.05$). TYR was negatively correlated with *novel.8169* and *novel.1732* ($P < 0.01$), but positively with *EVM0016022* ($P < 0.05$). *novel.8169* was positively associated with *novel.1732* ($P < 0.01$) and negatively with *EVM0016022* ($P < 0.05$). *novel.1732* was markedly negatively associated with *EVM0016022* ($P < 0.05$). *EVM0007771* was positively correlated with *EVM0014058* ($P < 0.01$) and *EVM0024005*, *EVM0022607* ($P < 0.05$). *EVM0016022* and *EVM0014058* were remarkably positively correlated with *EVM0024005* ($P < 0.05$) and *EVM0014058* with *EVM0022607* ($P < 0.05$). Flavonoid content was positively associated with *novel.8169* and *novel.1732*, but negatively with *EVM0004153*, *EVM0007771*, *EVM0016022*, *EVM0014058*, *EVM0024005*, and *EVM0022607* (no marked correlation). These findings provide insights into the molecular mechanisms underlying the impact of AS treatment in delaying browning in fresh-cut taro.

4. Discussion

Fresh-cut fruit and vegetables are highly susceptible to mechanical damage during processing, leading to oxidation and browning, significantly compromising their sensory and nutritional value [39]. Our study demonstrated that AS treatment maintained higher hardness and GSH content in fresh-cut taro compared to the CK group. Notably, AS treatment reduced weight loss and browning, enhanced APX and GR enzyme activities, decreased flavonoids and reducing sugar contents, and attenuated the accumulation of O_2^- and H_2O_2. The activities of TYR and LOX enzymes were also inhibited over the CK group, resulting in superior storage quality. These observations align with previous studies showing that AS enhanced antioxidant capacity in fresh-cut apples [40]. Therefore, AS treatment effectively preserves the storage quality of fresh-cut taro.

Chemical preservation of fresh-cut fruit and vegetables using antioxidants and preservatives is a common method that offers effective results. However, the presence of chemical preservatives or pigment residues has sparked concerns over food safety. In contrast, AA, a natural antioxidant with high safety, is commonly used as a color preservative to prevent browning. Additionally, US, a physical processing technique, offers safety, convenience, and energy efficiency, making it suitable for color protection and preservation of fresh-cut produce [41]. Our findings indicate that the combined AS treatment maintains the storage quality and safety of fresh-cut taro, echoing previous studies that reported US inhibiting PPO activity and enhancing the storage quality of fresh-cut red cabbages [42].

GO function and KEGG pathway analyses of the DEGs in fresh-cut taro revealed evident enrichment in photosynthesis, ER protein processing, and isoflavone biosynthesis after 12 d in both the treated and CK groups, aligning with the GO enrichment results. Browning, a color change resulting from oxidation, is often influenced by oxidase activity.

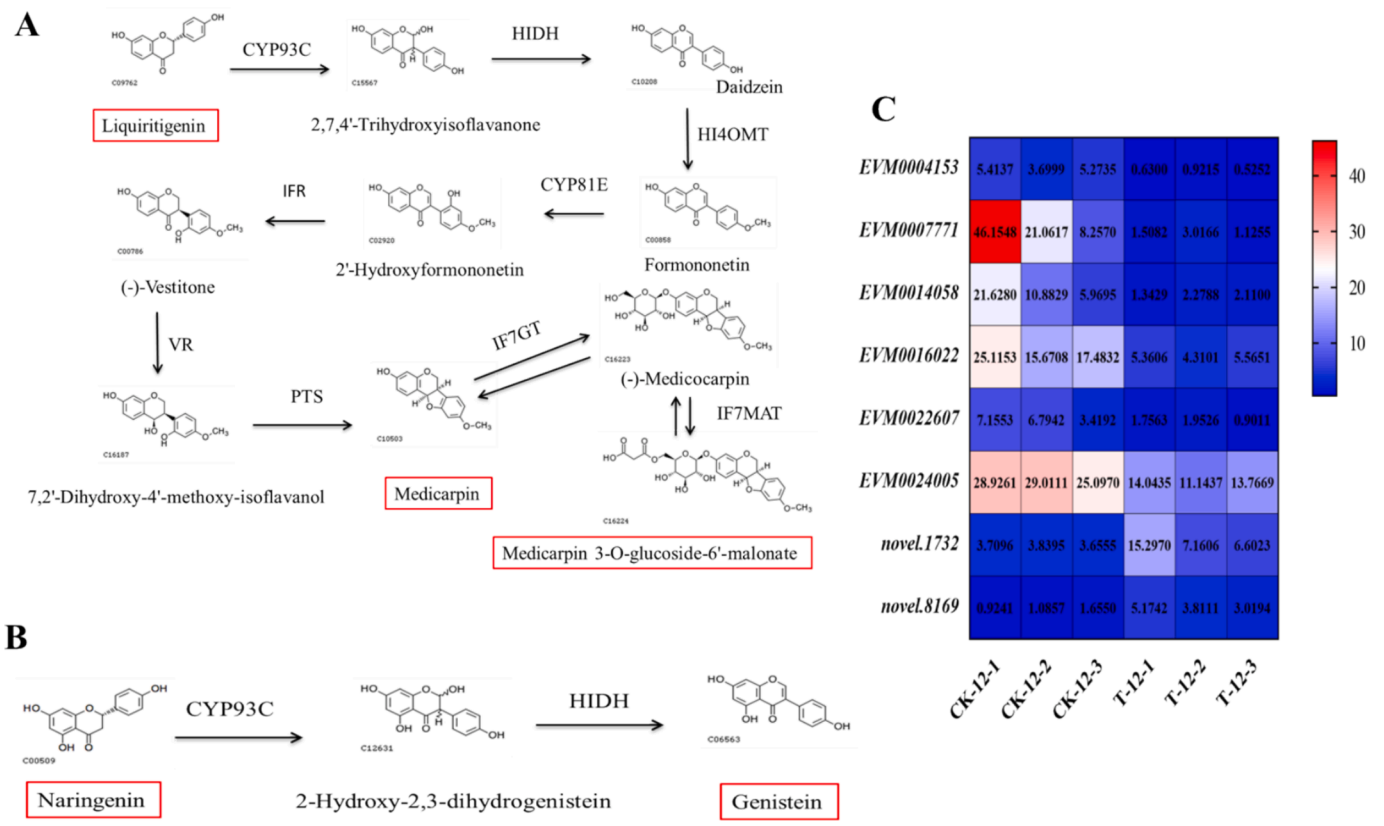

Fig. 12. Heat maps of the isoflavone biosynthesis pathways and differentially expressed genes (DEGs) in the AS and CK groups at 12 d. A and B: isoflavone biosynthesis pathway, the compounds in the red box are essential reactants and products in this process; C: A calorimetric map of the DEGs. In Figure C, the more intense the red color, the higher the gene expression, and the more intense the blue color, the lower the gene expression. (For interpretation of the references to color in this figure legend, the reader is referred to the web version of this article.)

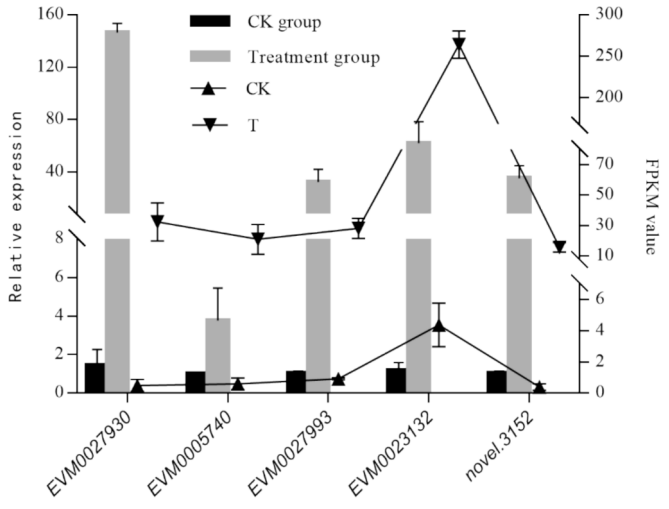

Fig. 13. qRT-PCR-based verification of the differentially expressed genes (DEGs) in fresh-cut taro on 12 d. The DEGs in the protein processing pathway on the endoplasmic reticulum of fresh-cut taro with (treatment group) or without AS treatment (CK group) on 12 d (transcriptome sequencing results). CK: the control group and T: AS treatment group (qRT-PCR results).

Altered photosynthesis may impact intracellular metabolic activities, including oxidase activity. Therefore, the down-regulated expression of the D2 protein in the photosystem II P680 reaction center could be associated with the activity of oxidation-related enzymes in fresh-cut taro, potentially promoting browning-associated reactions.

In the ER protein processing pathway [43], the expression of the protein glycosyltransferase-encoding gene was up-regulated in the treatment groups compared to CK, indicating an increased demand for glycosylation modification in the cells of fresh-cut taro. This effect may be due to cell damage from cutting or the physiological responses to external stimuli. Enhanced glycosyltransferase expression aids in maintaining cell homeostasis during these physiological changes. Protein glycosyltransferase plays a role in various biological processes [44], and its upregulation may influence browning-related signaling pathways in fresh-cut taro. Glycosylation can modulate the activity of antioxidant enzymes, thereby affecting the resistance of cells to oxidative damage and, subsequently, the browning degree of fresh-cut taro. AA, a potent antioxidant, scavenges free radicals and inhibits oxidation. Coupled with US treatment, AA may more efficiently eliminate intracellular free radicals, reduce oxidative damage, and mitigate browning. US treatment may enhance the cellular penetration of AA, boosting its antioxidant effects. Additionally, US may modulate protein glycosyltransferase activity, inhibiting browning. While the up-regulation of glycosyltransferase is associated with browning in fresh-cut taro, AS treatment may inhibit this process through multiple mechanisms. However, further research is necessary to elucidate the precise browning-related mechanisms and inhibition-associated principles in fresh-cut taro.

Flavonoids, natural pigments abundant in plants, exhibit antioxidant properties. However, their content in post-harvest fruit markedly declines under low-temperature storage, contrasting with normal temperature conditions [10]. Excessive flavonoids can induce browning in fresh-cut taro, compromising its visual appeal and taste. While the enhanced biosynthesis and release of flavonoids protect fresh-cut taro from damage caused by cutting or squeezing, they also ward off external microorganisms and oxidative stress. However, excessive flavonoid content can cause tissue damage, leading to browning. Suppressing the

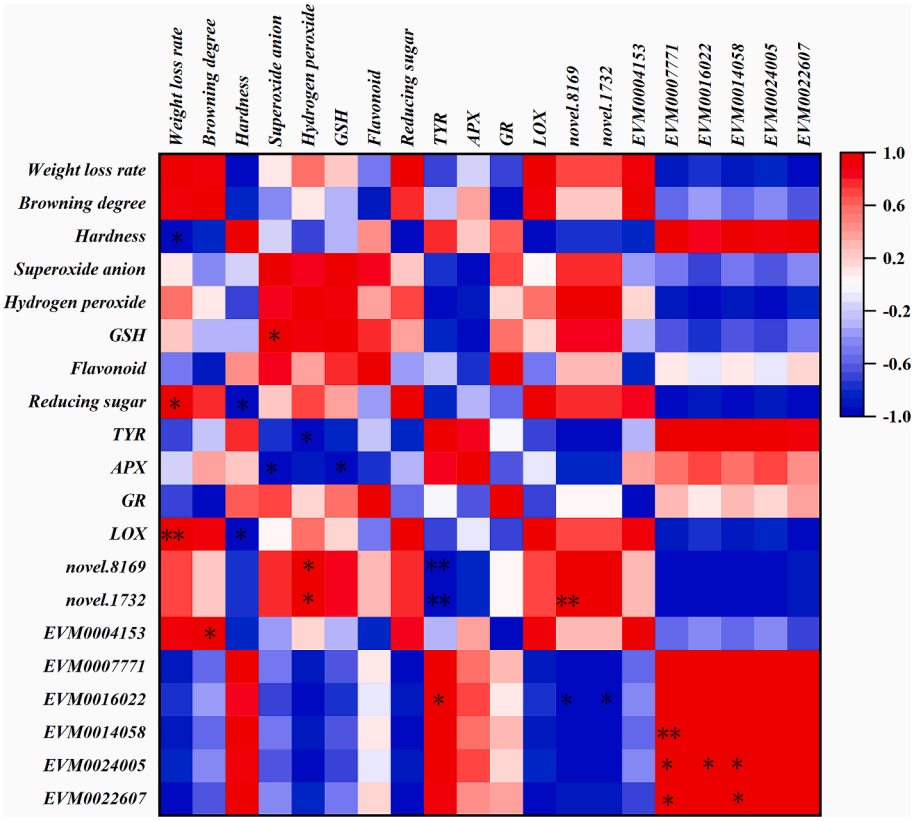

Fig. 14. Pearson correlation analysis matrix between the physiological traits and differentially expressed genes in the isoflavone biosynthesis pathway. *Significant correlation ($P < 0.05$); **Highly significant correlation ($P < 0.01$).

accumulation of flavonoids can mitigate browning in fresh-cut taro, which was consistent with our experimental findings (Fig. 5B). The AS treatment group exhibited lower flavonoid content compared to the CK group. Transcription analysis showed that two DEGs were up-regulated on 12 d, six were down-regulated, and seven were down-regulated on 20 d. Biotechnology-based modulation of plant extracts and antioxidants can be employed to curtail flavonoid biosynthesis or contents. For instance, gene editing techniques can target flavonoid biosynthesis-related genes, while specific plant extracts can hinder flavonoid release. Additionally, antioxidants can be introduced during taro storage and processing to minimize flavonoid-induced browning. In conclusion, suppressing flavonoid accumulation may attenuate browning in fresh-

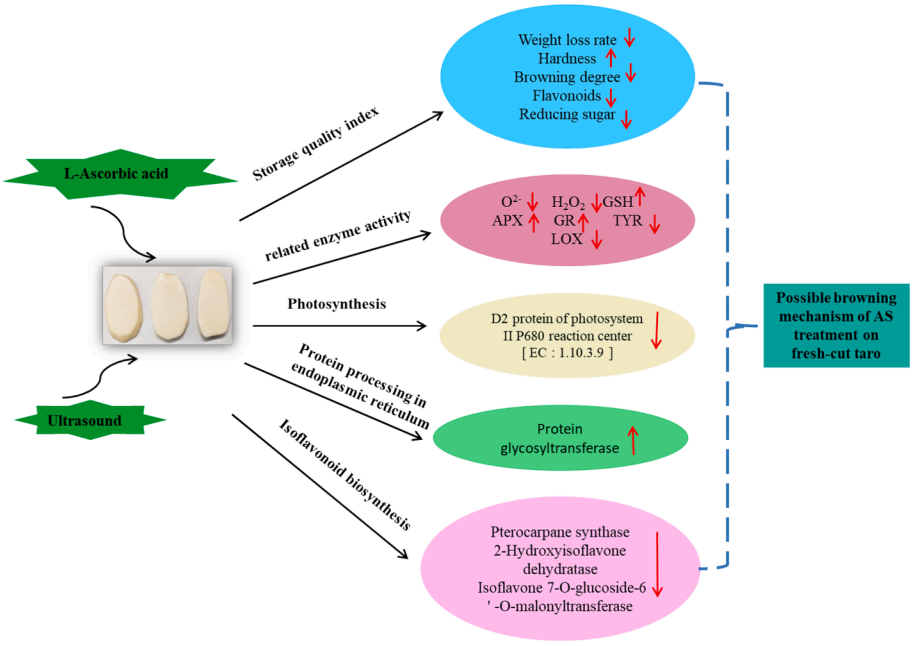

Fig. 15. Possible mechanism underlying the delay in the browning of fresh-cut taro AS treatment. Up arrows indicate high values or enhanced gene expression, while down arrows represent low values or suppressed gene expression.

cut taro, though further research is needed to elucidate its specific effects. Multiple strategies can be utilized in practical applications to reduce flavonoid content and enhance the storage quality of fresh-cut taro.

In summary, AS treatment may safeguard photosynthesis, ER protein processing, and isoflavone biosynthesis by alleviating oxidative stress, thus mitigating browning-related reactions in fresh-cut taro. These pathways are crucial in browning and color preservation. Consequently, the map explaining the possible mechanism underlying the delay in the browning of fresh-cut taro by AS treatment was obtained (Fig. 15). Elucidating these mechanisms could facilitate the development of more efficient preservation techniques, enhancing the quality and nutritional value of fresh-cut taro. Future studies should delve deeper into the specific mechanisms of the pathways associated with fresh-cut taro preservation and explore strategies to improve its storage quality through pathway modulation.

5. Conclusions

After CK and AS treatment, the storage quality of fresh-cut taro exhibited significant differences. AS treatment effectively reduced weight loss and browning, maintained hardness, suppressed O_2^- and H_2O_2 accumulation, enhanced GSH levels, curbed flavonoids and reducing-sugars accumulation, sustained higher APX and GR activities, and inhibited TYR and LOX activities, thereby enhancing sensory quality. Using Illumina high-throughput sequencing, we sequenced 15 fresh-cut taro samples, revealing 45,935 DEGs, including 27,132 up-regulated and 18,803 down-regulated genes. GO and KEGG analysis indicated that AS treatment down-regulated the genes related to photosynthesis and isoflavone biosynthesis while up-regulating those linked to protein processing in the endoplasmic reticulum at 12 d. This study enhances our understanding of the post-harvest physiology of fresh-cut taros and offers valuable insights into the development of their storage and preservation technology.

Author contributions

Lin Chen and Lulu Chu designed the experiments. Lin Chen and Lili Chen performed the experiments. Lin Chen and Bingzhi Chen analyzed the data and drafted the manuscript. Luyu Xie, Youjin Deng, and Yuji Jiang reviewed and edited the manuscript. All authors read and approved the final manuscript.

CRediT authorship contribution statement

Lin Chen: Visualization, Validation, Software, Project administration, Methodology, Investigation. **Bingzhi Chen:** Writing – review & editing, Visualization, Methodology, Investigation, Formal analysis, Data curation, Conceptualization. **Lulu Chu:** Supervision, Software, Resources, Project administration, Methodology. **Lili Chen:** Visualization, Validation, Software, Project administration, Methodology, Investigation. **Luyu Xie:** Writing – review & editing, Visualization, Validation, Supervision, Software. **Youjin Deng:** Resources, Investigation, Funding acquisition, Formal analysis, Data curation. **Yuji Jiang:** Writing – review & editing, Visualization, Validation, Supervision, Methodology, Funding acquisition, Formal analysis, Data curation, Conceptualization.

Declaration of competing interest

The authors declare that they have no known competing financial interests or personal relationships that could have appeared to influence the work reported in this paper.

Acknowledgments

This study was supported by the Fujian Provincial Association of Science and Technology Yongdingyu Science and Technology Courtyard (Agricultural Technology Association issued words [2023] No. 23).

Appendix A. Supplementary data

Supplementary data to this article can be found online at https://doi.org/10.1016/j.ultsonch.2024.107178.

Data Availability

Data will be made available on request.

References

[1] A. Bari, P. Giannouli, Gelatin and Gelatin/Rice Starch Coatings Affect Differently Fresh-Cut Potatoes and Colocasia Slices[J], Processes 11 (8) (2023), https://doi.org/10.3390/pr11082383.
[2] A. Baselice, F. Colantuoni, A.D. Lass, et al., Trends in EU consumers' attitude towards fresh-cut fruit and vegetables[J], Food Qual. Prefer. (2017) 5987–5996, https://doi.org/10.1016/j. foo-dqual.2017.01.008.
[3] M.C. Giannakourou, T.N. Tsironi, Application of Processing and Packaging Hurdles for Fresh-Cut Fruit and Vegetables Preservation[J], Foods 10 (4) (2021) 830, https://doi.org/10.3390/foods10040830.
[4] B. Wang, Y. Huang, Z. Zhang, et al., Ferulic acid treatment maintains the quality of fresh-cut taro (Colocasia esculenta) during cold storage[J], Front. Nutr. 9 (2022) 884844, https://doi.org/10.3389/fnut.2022.884844.
[5] X. Yanhui, Z. Jieli, J. Yuanyuan, et al., Cinnamic acid treatment reduces the surface browning of fresh-cut taro[J], Sci. Hortic. (2022) 110613, https://doi.org/10.1016/j.scienta.2021.
[6] W. Bin, W. Yukun, H. Yongyan, et al., Anti-browning effects of citronellal on fresh-cut taro (Colocasia esculenta) slices under cold storage condition [J], Front. Sustainable Food Syst. 6 (2022), https://doi.org/10.3389/fsufs.2022.1001362.
[7] X. Yuan, T. Binglin, W. Yukun, et al., Inhibitory effects of peppermint extracts on the browning of cold-stored fresh-cut taro and the phenolic compounds in extracts [J], Front. Sustainable Food Syst. 7 (2023) 1191396, https://doi.org/10.3389/fsufs.2023.1191396.
[8] X. Yanhui, H. Jinming, Z. Jian, et al., Application of citronella and rose hydrosols reduced enzymatic browning of fresh-cut taro[J], J. Food Biochem. 44 (8) (2020) e13283, https://doi.org/10.1111/jfbc.13283.
[9] M.M. Tosif, A. Bains, G. Goksen, et al., Application of Taro (Colocasia esculenta) Mucilage as a Promising Antimicrobial Agent to Extend the Shelf Life of Fresh-Cut Brinjals (Eggplants)[J], Gels 9 (11) (2023), https://doi.org/10.3390/gels9110904.
[10] S. Guo, D. Wang, Y. Ma, et al., Combination of RNA-Seq transcriptomics and iTRAQ proteomics reveal the mechanism involved in fresh-cut yam yellowing[J], Sci. Rep. 11 (1) (2021) 7755, https://doi.org/10.1038/s41598-021-87423-4.
[11] W. Jian, Z. Jiazhen, L. Xiaofen, et al., Transcriptome analysis reveals mechanisms of acetylsalicylic acid-mediated fruit quality maintenance in fresh-cut kiwifruit[J], Post-Harvest Biol. Tech. 194 (2022), https://doi.org/10.1016/j.postharvbio.2022.112100.
[12] J. Wenwen, Z. Dan, Z. Longgang, et al., l-Cysteine Treatment Delayed the Quality Deterioration of Fresh-Cut Button Mushrooms by Regulating Oxygen Metabolism, Inhibiting Water Loss, and Stimulating Endogenous Hsub2/subS Production.[J], J. Agric. Food Chem. 71 (1) (2022), https://doi.org/10.1021/acs.jafc.2c06795.
[13] W. Lihua, W. Wenjun, W. Qingjun, et al., Transcriptome-wide N6-methyladenosine (m6A) methylation profiling of fresh-cut potato browning inhibition by nitrogen [J], Post-Harvest Bio. Technol. 187 (2022), https://doi.org/10.1016/j.postharvbio.2022.111870.
[14] Y. Wang, N. Yuan, Y. Guan, et al., Transcriptomic Analysis Reveals the Mechanism of Lignin Biosynthesis in Fresh-Cut Cucumber[J], Horticulturae 9 (4) (2023), https://doi.org/10.3390/horticul-turae9040500.
[15] C. Peitao, L. Jiaxin, L. Qingqing, et al., Transcriptome and physiological analysis revealed the difference of resistance to fresh-cut browning among sweetpotato genotypes[J], Post-Harvest Biol. Technol. 205 (2023), https://doi.org/10.1016/j.postharvbio.2023.112504.
[16] C. Jingxin, W. Ankang, Y. Mingliang, et al., Characterization of sodium alginate-based films incorporated with thymol for fresh-cut apple packaging[J], Food Control 126 (2021), https://doi.org/10.1016/j.foodcont.2021.108063.
[17] C. Liu, C. Chen, A. Jiang, et al., Effects of plasma-activated water on microbial growth and storage quality of fresh-cut apple[J], Innov. Food Sci. Emerg. Technol. 59 (C) (2019) 102256, https://doi.org/10.1016/j.ifset.2019.102256.
[18] E. Badin, Y. Rossi, M. Montenegro, et al., Thermal processing of raspberry pulp: Effect on the color and bioactive compounds[J], Food Bioprod. Process. (2020) 124469–124477, https://doi.org/10.1016/j.fbp.2020.08.016.
[19] S. Luyi, Y. Hui, C. Shuai, et al., Combination effects of ultrasound and citral nanoemulsion against Shigella flexneri and the preservation effect on fresh-cut carrots[J], Food Control 155 (2024), https://doi.org/10.1016/j.foodcont.2023.110069.

[20] L. Ma, M. Zhang, B. Bhandari, et al., Recent developments in novel shelf life extension technologies of fresh-cut fruit and vegetables[J], Trends Food Sci. Technol. (2017) 6423–6438, https://doi.org/10.1016/j.tifs.2017.03.005.
[21] W. Yajing, L. Yuexin, Y. Shuhan, et al., Gaseous ozone treatment prolongs the shelf-life of fresh-cut kiwifruit by maintaining its ascorbic acid content[J], LWT 172 (2022), https://doi.org/10.1016/j.lwt.2022.114196.
[22] Z. Lijuan, H. Wanfeng, M. Ayesha, et al., Browning inhibition in fresh-cut Chinese water chestnut under high pressure COsub2/sub treatment: Regulation of reactive oxygen species and membrane lipid metabolism[J], Food Chem. (2023) 427136586–428136586, https://doi.org/10.1016/j.foodchem.2023.136586.
[23] J. Li, J. Shi, X. Huang, et al., Effects of pulsed electric field pretreatment on frying quality of fresh-cut lotus root slices[J], LWT 132 (2020), https://doi.org/10.1016/j.lwt.2020.109873.
[24] C. Chen, L. Lin, W. Yang, et al., An Updated Organic Classification of Tyrosinase Inhibitors on Mela-nin Biosynthesis[J], Curr. Org. Chem. 19 (1) (2014) 4–18, https://doi.org/10.2174/13852728196661411072248O6.
[25] X. Ru, N. Tao, Y. Feng, et al., A novel anti-browning agent 3-mercapto-2-butanol for inhibition of fresh-cut potato browning[J], Post-Harvest Biol. Technol. 170 (2020), https://doi.org/10.1016/j.postharvbio.2020.111324.
[26] Z. Fuhui, X. Dongying, X. Siguo, et al., Inhibition of wound healing in fresh-cut potatoes by ascorbic acid is associated with control of the levels of reactive oxygen species and the AsA-GSH cycle[J], Sci. Hortic. 323 (2024), https://doi.org/10.1016/j.scienta.2023.112472.
[27] S. Chen, Y. Zhou, Y. Chen, et al., Fastp: An ultra-fast all-in-one FASTQ preprocessor [J], Bioinformatics 34 (2018) i884–i890, https://doi.org/10.1093/bioinformatics/bty560.
[28] X. Mao, T. Cai, J.G. Olyarchuk, et al., Automated genome annotation and pathway identification using the KEGG Orthology (KO) as a controlled vocabulary[J], Bioinformatics 21 (19) (2005) 3787–3793, https://doi.org/10.1093/bioinformatics/bti430.
[29] D. Kim, B. Langmead, S.L. Salzberg, HISAT: a fast spliced aligner with low memory requirements[J], Nat. Methods 12 (4) (2015) 357–360, https://doi.org/10.1038/nmeth.3317.
[30] T. Min, Y. Bao, B. Zhou, et al., Transcription Profiles Reveal the Regulatory Synthesis of Phenols du-ring the Development of Lotus Rhizome (Nelumbo nucifera Gaertn)[J], Int. J. Mol. Sci. 20 (11) (2019) 2735, https://doi.org/10.3390/ijms20112735.
[31] J. Zecheng, L. Rui, T. Yue, et al., Transcriptome Analysis Reveals the Inducing Effect of Bacillus siamensis on Disease Resistance in Postharvest Mango Fruit[J], Foods 11 (1) (2022) 107, https://doi.org/10.3390/foods11010107.
[32] C. Chichang, W. Ye, X. Li, et al., Characterization of Abscisic Acid and Ethylene in Regulating the White Blush in Fresh-Cut Carrots[J], Int. J. Mol. Sci. 23 (21) (2022) 12788, https://doi.org/10.3390/ijms232112788.
[33] M.I. Love, W. Huber, S. Anders, Moderated estimation of fold change and dispersion for rna-seq data with deseq2[J], Genome Biol. 15 (2014), https://doi.org/10.1186/s13059-014-0550-8.
[34] M. Ashburner, C.A. Ball, J.A. Blake, et al., Gene ontology: Tool for the unification of biology. The gene ontology consortium, Nat. Genet. 25 (2000) 25–29, https://doi.org/10.1038/75556.
[35] H. Varet, L. Brillet-Guéguen, J.-Y. Coppée, et al., SARTools: A DESeq2- and EdgeR-based r pipeline for comprehensive differential analysis of RNA-seq data, PLoS One 11 (2016) e0157022, https://doi.org/10.1371/journal.pone.0157022.
[36] C. Jingxin, M. Linchun, L. Wenjing, et al., Transcriptome profiling of post-harvest strawberry fruit in response to exogenous auxin and abscisic acid.[J], Planta 243 (1) (2016) 183–197, https://doi.org/10.1016/j.postharvbio.2023.112504.
[37] L. Suping, H. Jingyu, N. Shiqi, et al., Bacillus velezensis HY19 as a sustainable preservative in post-harvest citrus (Citrus reticulata Blanco L.) fruit management [J], Food Control 155 (2024), https://doi.org/10.1016/j.foodcont.2023.110068.
[38] C. Zhang, Y. Xin, Z. Wang, et al., Melatonin-induced myeloblastosis viral oncogene homologs alleviate fresh-cut lotus root browning during storage by attenuating flavonoid biosynthesis and reactive oxygen species[J], J. Sci. Food Agric. 103 (11) (2023) 5452–5461, https://doi.org/10.1002/jsfa.12619.
[39] Z. Zhuping, T. Rui, W. Chuang, et al., Riboflavin inhibits browning of fresh-cut apples by repressing phenolic metabolism and enhancing antioxidant system[J], Post-Harvest Biol. Technol. 187 (2022), https://doi.org/10.1016/j.postharvbio.2022.111867.
[40] S.K. Mahmoud, D. Hosain, Z. Lolav, et al., Shelf-life enhancement and microbial load reduction of fresh-cut apple using ascorbic acid and carboxymethyl cellulose coating combined with ultrasound treatment.[J], Food Sci. Technol. Int. (2023), https://doi.org/10.1177/10820132231206415.
[41] F.M. Pintos, M.L. Lemoine, G.E.G. Grozeff, et al., Use of riboflavin to reduce decay and extend the shelf-life of fresh-cut sweet pepper[J], Post-Harvest Biol. Technol. 188 (2022), https://doi.org/10.1016/j.postharvbio.2022.111882.
[42] H. Chen, Z. HongChang, Z. YiMing, et al., Ultrasonic washing as an abiotic elicitor to induce the accumulation of phenolics of fresh-cut red cabbages: Effects on storage quality and microbial safety.[J], Front. Nutr. 9 (2022) 1006440, https://doi.org/10.3389/fnut.2022.
[43] Z. Lei, X. Fangxu, Transcriptome analysis of fresh-cut kiwifruit treated with slightly acidic electrolyzed water (SAEW) and 1-methylcyclopropene (1-MCP)[J], Plant Growth Reg. 101 (3) (2023) 811–822, https://doi.org/10.1007/s10725-023-01058-1.
[44] J. Liu, C. Feng, M. Liu, et al., An immune-related multi-omics analysis of dolichyl-diphosphooligosaccharide protein glycosyltransferase in glioma: prognostic value exploration and competitive endogenous RNA network identification[J], IET Syst. Biol 17 (5) (2023) 271–287, https://doi.org/10.1049/syb2.12075.